Remotely triggered seismicity in north China following the 2008 M_w 7.9 Wenchuan earthquake

Zhigang Peng[1], Weijun Wang[2], Qi-Fu Chen[2], and Tao Jiang[1,3]

[1]School of Earth and Atmospheric Sciences, Georgia Institute of Technology, Atlanta, GA, 30332
[2]Institute of Earthquake Science, China Earthquake Administration, Beijing, China
[3]College of Instrumentation Science and Electrical Engineering, Jilin University, Changchun, Jilin, China

(Received October 9, 2008; Accepted March 9, 2009; Online published January 26, 2011)

We conduct a systematic survey of remote triggering of earthquakes in north China following the 2008 M_w 7.9 Wenchuan earthquake. We identify triggered earthquakes as impulsive seismic energies with clear P and S arrivals on 5 Hz high-pass-filtered three-component velocity seismograms during and immediately after the passage of teleseismic waves. We find clearly triggered seismic activity near the Babaoshan and Huangzhuang-Gaoliying faults southwest of Beijing, and near the aftershock zone of the 1976 M_w 7.6 Tangshan earthquake. While several earthquakes occur during and immediately after the teleseismic waves in the aftershock zone of the 1975 M_w 7.0 Haicheng earthquake, the change of seismicity is not significant enough to establish the direct triggering relationship. Our results suggest that intraplate regions with active faults associated with major earthquakes during historic or recent times are susceptible to remote triggering. We note that this does not always guarantee the triggering to occur, indicating that other conditions are needed. Since none of these regions is associated with any active geothermal or volcanic activity, we infer that dynamic triggering could be ubiquitous and occur in a wide range of tectonic environments.

Key words: Dynamic triggering, the 2008 Wenchuan earthquake, earthquake interaction.

1. Introduction

It is well known that earthquakes interact with each other. For example, large shallow earthquakes are typically followed by increased seismic activity in nearby regions, known as "aftershocks" (e.g., Utsu *et al.*, 1995). However, only recently seismologists started to realize that large earthquakes could also cause a significant increase of seismic activity in regions that are several hundreds to thousands of kms away (e.g., Hill *et al.*, 1993; Brodsky *et al.*, 2000; Gomberg *et al.*, 2001; Hough and Kanamori, 2002; Kilb *et al.*, 2002; Hough *et al.*, 2003; Gomberg *et al.*, 2004; Prejean *et al.*, 2004; Freed, 2005; Hill and Prejean, 2007; Velasco *et al.*, 2008). Because static stresses resulting from fault displacements fall off more rapidly and become negligible beyond several hundred kms (e.g., Freed, 2005), the elevated seismicity at large distances is generally considered as "remotely triggered" by the dynamic stresses during the passage of seismic waves generated by large earthquakes. Since the immediate cause of these triggered events is apparent and relatively easy to quantify, systematic analysis of remote triggering offers a unique opportunity for better understanding the underlying mechanism of earthquake interaction and physics of earthquake occurrence.

So far most of the remotely triggered earthquakes are identified near active plate boundary faults with abundant background seismicity (e.g., Hill *et al.*, 1993; Gomberg *et al.*, 2001; Prejean *et al.*, 2004). Only a few studies have found remotely triggered earthquakes in relatively stable intraplate regions (e.g., Hough *et al.*, 2003; Gomberg *et al.*, 2004). Recently, Velasco *et al.* (2008) conducted a systematic global survey of microearthquakes triggered by many large earthquakes. They found that earthquake triggering is a ubiquitous phenomenon that is independent of the tectonic environment of the main earthquake or the triggered event. Their study motivated us to search for further evidence of remote triggering in intraplate regions to better understand the necessary conditions that favor dynamic triggering.

The 2008/05/12 M_w 7.9 Wenchuan earthquake offers a unique opportunity to conduct such study. This earthquake occurred in Eastern Sichuan, China, and ruptured predominately northeastwards for ~250 km along the Longmenshan fold-and-thrust belt that bounds the Tibetan plateau and the Sichuan basin (Burchfiel *et al.*, 2008). The main event and its rigorous aftershock sequences were recorded by many permanent and temporary seismic stations deployed by the China Earthquake Administration (CEA).

We focus in this study on triggered seismic activity around the Beijing metropolitan area and the southern portion of the Liaoning Province in north China (Fig. 1) for the following reasons. First, this region is covered by dense regional seismic network. The Beijing metropolitan digital Seismic Network (BSN) provides coverage around Beijing and nearby areas (Chen *et al.*, 2006). Currently, this network consists of 107 broadband, borehole and surface short-period stations. Second, this region is in the rupture propagation direction of the Wenchuan earthquake, and hence has a great potential for generating triggered seismic

doi:10.5047/eps.2009.03.006

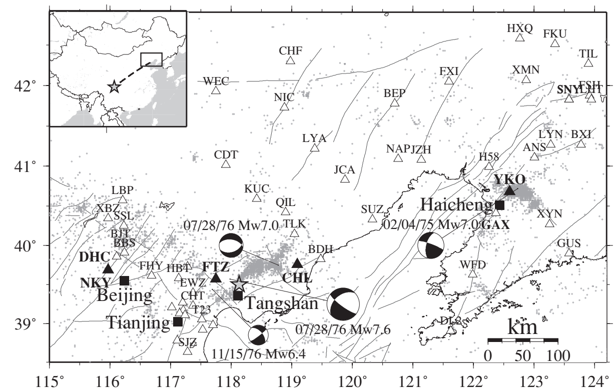

Fig. 1. A map showing the study area in north China. The open triangles mark the locations of stations that recorded the 05/12/2008 M_w 7.9 Wenchuan earthquake, and the black triangles mark the nearest and nearby stations that recorded the triggered earthquakes. The gray star marks the location of an $M_L = 1.3$ earthquake north of Tangshan occurred during the surface waves of the Wenchuan earthquake. The gray lines denote active fault traces. The focal mechanism solutions of the 1975 M_w 7.0 Haicheng earthquake, the 1975 M_w 7.6 Tangshan earthquake and its two large aftershocks are plotted. The small gray dots mark the background seismicity from 01/01/2001 to 11/30/2008. The inset shows map of China. The large star marks the epicenter of the M_w 7.9 Wenchuan earthquake. The box corresponds to the study area and the dashed line shows the ray path.

activity due to rupture directivity effect (e.g., Gomberg *et al.*, 2001, 2004). Finally, this area has been highly seismic active in 1960s and 1970s with 5 $M>7$ earthquakes, including the 1975 M_w 7.0 Haicheng and 1976 M_w 7.6 Tangshan earthquakes. These large earthquakes are followed by protracted aftershock activity that is currently visible. This allows us to compare the triggering potentials with varying background seismicity rate.

2. Analysis Procedure

We download continuous seismic data recorded by stations in the BSN and nearby regional seismic network 6 hour before and after the origin time of the Wenchuan mainshock (2008/05/12 06:28:01.57). We scan through all the records, and remove those bad traces with no seismic data or severely clipped during the surface waves of the Wenchuan earthquake. After the selection process, we obtain a total of 61 stations for further analysis.

Next, we visually identify earthquakes as impulsive seismic energies with clear P and S arrivals on 5 Hz high-pass-filtered three-component velocity seismograms, and compare events in the 6-hour time windows before and after the mainshock origin times. We also checked nearby stations to ensure that the identified earthquake signals are recorded by at least two stations. Since it is not practical to accurately determine the hypocentral locations of most events recorded at a few nearby stations, we estimate the approximate distance to the nearest station based on the travel time differences of P and S waves. We require that the S–P times of the identified events to be less than 15 s, roughly corresponding to a propagating distance of 120 km. Because this distance is much smaller than the distance to the epicenter of the Wenchuan earthquake, we use the location of the nearest station as a proxy for the location of identified earthquake.

To evaluate the significance of the seismicity rate changes, we first select from the regional earthquake catalogs all earthquakes 30 days before and after the occurrence of the Wenchuan event. We use the same spatial window of 120 km relative to the examined station, and select events with magnitude $m \geq 1.5$, which is at least 0.3 units larger than the magnitude of completeness estimated from the maximum curvature method (Woessner and Wiemer, 2005). Next, we compute a β statistic, which measures the difference between the observed number of events after the mainshock and the expected number based on the average seismicity rate before the mainshock, and scaled by the standard deviation of the seismicity rate (Matthews and Reasenberg, 1988; Reasenberg and Simpson, 1992). The β statistic is defined by

$$\beta(n_a, n_b; t_a, t_b) = \frac{n_a - E(n_a)}{\mathrm{Var}(n_a)} \qquad (1)$$

where n_b and n_a is the number of earthquakes observed before and after the mainshock, t_b and t_a is the time duration before and after the mainshock, respectively. For a Poisson process, $E(n_a) = \mathrm{Var}(n_a) = n_b(t_a/t_b)$ (Hill and Prejean, 2007). Results with $|\beta| > 2$ (approximately two standard deviations) are generally considered to be statistically significant (Reasenberg and Simpson, 1992; Hill and Prejean, 2007).

Finally, we manually pick earthquakes on the high-pass-filtered seismograms 6 hour before and 1 hour after the Wenchuan P arrival and compute the corresponding β statistic. The analysis procedure is similar to that used in Peng *et al.* (2007) to identify early aftershocks, and is briefly described here. First, we take the envelope function of the 5 Hz high-pass-filtered seismogram, smooth it by the half width of 50 point, and stack the resulting three-component envelopes to obtain the envelope function for each station. Next, we identify an event by searching for clear double peaks in the envelope that correspond to the P and S arrivals. We also compute the median value of the envelope function with duration of 1 hour before the Wenchuan P arrival, and use 9 times the median absolute deviation (MAD) as an amplitude threshold. Only events with amplitude larger than such threshold are used to compute the β statistic. The threshold is chosen to ensure that we only include events with large enough amplitudes so that they are unlikely to be caused by random fluctuations in the background noise.

Overall, we find three regions that show potential earthquake activity associated with the Wenchuan earthquake. We briefly describe the characteristic of the earthquake activity in each region below, followed by a summary of observations and discussions. We find no clear evidence of earthquake activity during the 1-hour time window at other sites we examine.

3. Triggered Seismicity around Beijing

Beijing is situated near the juncture of the Yinshan-Yanshan Mountain and North China Plain fault block (Deng *et al.*, 2003). The North China Plain is a region of Mesozoic-Cenozoic rift basins and uplift structures that are crosscut by NNE- and NWW-oriented conjugate fault zones (Liu *et al.*, 2007). Many large earthquakes have

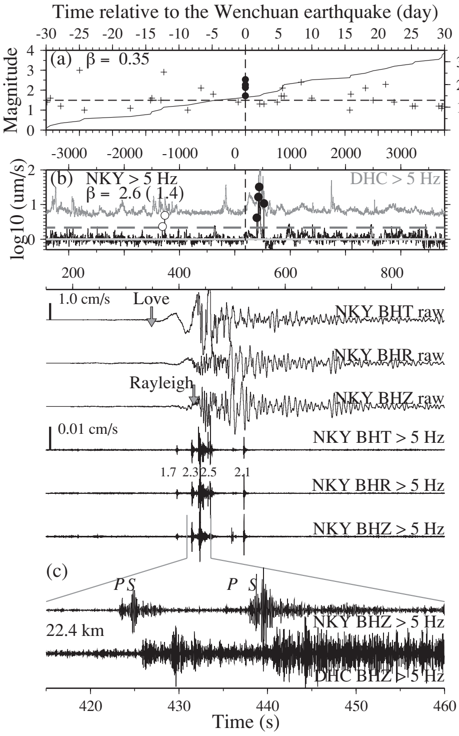

Fig. 2. (a) Seismicity within 30 days and 120 km of station NKY near Beijing. The solid line shows the cumulative number of events, and the solid circles mark the 4 events occurred during the passage of the surface waves. The horizontal dashed line marks the magnitude threshold of 1.5. The corresponding β statistic with $m \geq 1.5$ is 0.35. (b) The high-pass-filtered envelope functions at station NKY (solid line) and nearby station DHC (gray line; shifted up by 1.25 in $\log_{10}$ amplitude) within 1 hour of the P wave arrival of the Wenchuan earthquake (vertical dashed line). The horizontal gray and black dashed line marks the median and 9 times the median absolute deviation (MAD), which is used a threshold to pick seismic events. The open and solid circles mark the hand-picked events before and after the P arrival. The corresponding β statistic computed events within 6 hour and 1 hour before the P arrival 2.6 and 1.4, respectively. (c) The top three traces: the broadband three component (transverse, radial and vertical) seismograms recorded at station NKY. The middle three traces: 5 Hz high-pass-filtered seismograms showing small local earthquakes during the passage of surface waves. The corresponding local magnitudes of these events are also marked. The bottom two traces: zoom-in plots of the vertical seismograms showing the P and S waves of the two triggered earthquakes recorded at station NKY and a nearby station DHC with a distance of 22.4 km.

occurred near Beijing, including the 1679 $M \sim 8$ Sanhe-Pinggu earthquake and the 1976 M_w 7.6 Tangshan earthquake. The relocated seismicity (Li *et al.*, 2007) is generally associated with pre-existing faults imaged by wide-angle and deep seismic reflection profile. Figure 2 shows a comparison of the broadband and high-pass-filtered seismograms at station NKY about 35 km SW of Beijing. The Love waves generated by the Wenchuan mainshock arrived at ~390 s (with a nominal phase velocity of 4.3 km/s), and the Rayleigh waves arrived at ~430 s (with a nominal phase velocity of 3.5 km/s). After the 5 Hz high-pass filtering process, we identify at least 4 earthquakes during the passage of the large-amplitude surface waves. The first event occurred at around 385 s during the first cycle of the Love waves, and the rest three events occurred during the Rayleigh waves. The P and S waves are clearly shown in the three-component seismograms at station NKY, and

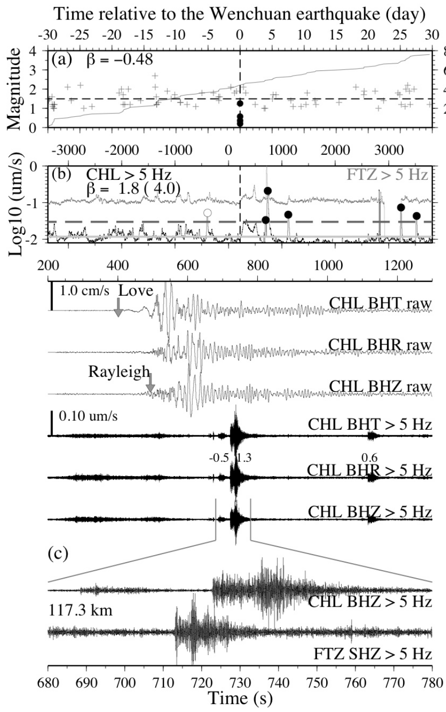

Fig. 3. (a) Seismicity within 30 days and 120 km of station CHL near the aftershock zone of the 1976 M_w 7.6 Tangshan earthquake. (b) The high-pass-filtered envelope functions at station CHL (solid line) and nearby station FTZ (gray line; shifted down by 2.2 in $\log_{10}$ amplitude) within 1 hour of the P wave arrival of the Wenchuan earthquake (vertical dashed line). (c) Raw and high-pass-filtered seismograms showing the teleseismic waves of the Wenchuan earthquake and locally generated seismic events, respectively. Other symbols and notations are the same as in Fig. 2.

could also be identified in the nearby station DHC. Due to lack of additional recordings, we were unable to actually locate these events. However, the S–P times are in the range of 1.1–1.7 s, roughly corresponding to propagation distance of 9–14 km, suggesting that these events must occur very close to station NKY. Finally, we estimate the local magnitude M_L of these events to be in the range of 1.7–2.5, based on the peak amplitude averaged over the two horizontal components and the S–P times. The magnitude computed here is likely a lower bound because of the 5 Hz high-pass-filtering. No magnitude correction is made in this study.

It is worth noting that none of these events were listed in the regional earthquake catalog. In addition, the seismicity rate from the catalog within 30 days of the Wenchuan earthquake does not show significant changes, with the β value of 0.35. However, the β value for the events picked from the 1-hour high-pass-filtered envelope function before and after the Wenchuan P arrival is 1.4. Since the β value depends on the duration of the time window, we also compute the β statistic using events identified from high-pass-filtered envelope functions with 6 hours before and 1 hour after the Wenchuan P arrival. The resulting β value is 2.6. Although these values are around 2, we still consider them as statistically significant, mainly because of the following reasons. First, the 4 events occurred during the arrivals of the large-amplitude surface waves, and the first event appears to be coincident with the arrival of the long-period Love waves, suggesting a possible correlation between the surface waves and the locally generated seismic events. Secondly, a direct examination of the high-pass-filtered envelope reveals that while there are a few small events that are above the threshold within 1 hour before the Wenchuan P arrival and after the passage of the surface waves, none of them has comparable amplitudes as those occurred during the surface waves of the Wenchuan event. Hence, we conclude that the 4 events are indeed triggered by the large-amplitude surface waves.

4. Triggered Seismicity around Tangshan

In 1976, the M_w 7.6 Tangshan earthquake occurred directly underneath the city of Tangshan, resulting in one of the most destructive events in term of the loss of life in human history. The mainshock ruptured a NE trending right-lateral strike-slip fault, which is clearly outlined by its aftershock sequence (Shedlock *et al.*, 1987) that is currently active (Fig. 1). We find possible triggered activity at stations north of Tangshan (Fig. 3). The seismic activity was initiated about 100 s after the passage of the large surface waves and continued for 2–3 hours. The largest seismic event occurred around 705 s after the origin time of the mainshock, and is clearly observed at nearby stations FTZ, BAD, CHL, TLK and KUC. Based on the hand-picked P arrival times and a 1D velocity model (Li *et al.*, 2007), we locate this earthquake to be at 118.13°E, 39.50°N with a horizontal error of 3.1 km. The hypocentral depth is 7.0±2.8 km. This places the triggered earthquake near the southern segment of the Tangshan aftershock zone. The corresponding M_L for this event is 1.3. Another two small earthquakes occurred around 680 s and 1200 s after the mainshock. We were unable to locate these events due to relatively small number of observations. Again, none of these events are listed in the regional earthquake catalog, and the β value from events within 30 days of the Wenchuan earthquake is only -0.48. In comparison, the β value from the high-pass-filtered envelope functions at station CHL is 4 with 1-hour time window before and after the Wenchuan P arrival. The β value drops to 1.8 within 6-hour time window before the Wenchuan P arrival. A direct examination of high-pass-filtered envelope reveals that although there are some fluctuations in the envelope amplitude before the mainshock, most of them are not associated with earthquakes because we were unable to identify clear P and S arrivals, and they are not coherent at nearby stations. In addition, none of them has comparable amplitudes as the M 1.3 event occurred immediately after the passage of the surface waves. Hence, we also consider the triggering effect near the Tangshan aftershock zone as statistically significant.

5. Triggered Seismicity around Haicheng

The M_w 7.0 1975 Haicheng earthquake is well known because it is considered to be the only major earthquake ever to be officially predicted (Wang *et al.*, 2006). This earthquake ruptured a northwest-trending left-lateral strike-slip fault, which is also evident from the current seismicity around this region (Fig. 1). Similar to what has been observed around the Tangshan aftershock zone, we also identified potential earthquake activity around the Haicheng area during the Wenchuan earthquake (Fig. 4). In comparison

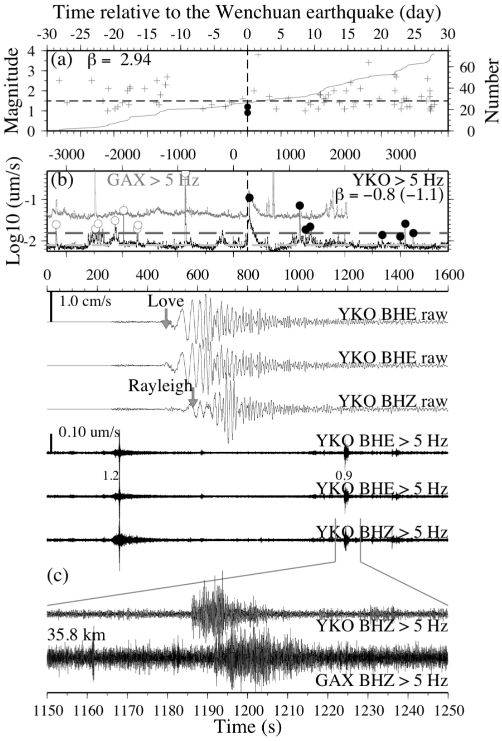

Fig. 4. (a) Seismicity within 30 days and 120 km of station YKO near the aftershock zone of the 1975 M_w 7.0 Haicheng earthquake. (b) The high-pass-filtered envelope functions at station YKO (solid line) and nearby station GAX (gray line; shifted up by 0.5 in $\log_{10}$ amplitude) within 1 hour of the P wave arrival of the Wenchuan earthquake. (c) Raw and high-pass-filtered seismograms showing the teleseismic waves of the Wenchuan earthquake and locally generated seismic events, respectively. Other symbols and notations are the same as in Fig. 2.

to the near instantaneous triggering of seismic activity during the surface waves at other stations (Figs. 2 and 3), we identify an event occurred at ~300 s during the passage of the P wave of the Wenchuan earthquake. This event is relatively small and was not recorded by the nearby station GAX. No clear seismic activity is shown during the large surface waves between 450 and 900 s. There are several seismic events showing up at around 1200–1400 s immediately after the passage of surface waves. Some of them are large enough to be recorded by the nearby station GAX.

The β value from earthquakes within 30 days of the Wenchuan earthquake is 2.94, which is larger than the previous two cases, and is considered as significant (Reasenberg and Simpson, 1992; Hill and Prejean, 2007). However, the β value from the 1-hour high-pass-filtered seismograms is only -1.1. If we increase the analyzed pre-mainshock time window to 6 hours, the β value is still negative. This is mainly because there are quite significant high-frequency energies before the mainshock, some of them have comparable and even larger amplitudes than those we identified during the P and immediately after the surface waves. Because of this, we were unable to establish a direct triggering relationship between the observed seismic activity near the Haicheng aftershock zone and the Wenchuan earthquake.

6. Summary and Discussions

Our study provides additional clear evidence of dynamic triggering within intraplate regions. Overall, we have identified three places in north China with clearly seismic activity during and immediately after the passage of teleseismic waves of the 2008 M_w 7.9 Wenchuan earthquake. In the first two cases near Beijing and within the Tangshan aftershock zone, we have confirmed that the triggering effect is statistically significant by computing the β statistic from earthquakes identified from high-pass-filtered seismograms. In the last case near the Haicheng aftershock zone, the seismic activity before the mainshock was relatively high, and we did not observe clear increase of seismicity during and immediately after the Wenchuan earthquake. Hence, the observed seismic events near Haicheng during the P wave and immediately after the surface waves probably occurred by random chance, rather than triggered by the Wenchuan earthquake.

Our study region is in the northern part of the North China Plain, which is an active basin formed under a pull-apart condition and crosscut by many conjugate faults in the NNE and NWW directions (Deng *et al.*, 2003). This is consistent with the focal mechanism solutions of moderate and large earthquakes in this region (Fig. 1). Hence, our study area can be best categorized as an intraplate transtensional tectonic regime. While the GPS measurements of crustal movement in north China is on the order of a few mm/yr or less (Wang *et al.*, 2001), elevated seismic activity during 1960s and 1970s with several large damaging earthquakes (including the 1975 Haicheng and 1976 Tangshan earthquakes) suggests that this region is seismically active. Our results are generally consistent with previous observations that remote triggering of microearthquakes is mostly observed at tectonically active extensional and transtensional regimes, although this picture could be partially biased by the uneven sampling in different tectonic regimes (e.g., Hill and Prejean, 2007).

Hough *et al.* (2003) conducted a survey of remote triggering in stable eastern US after the 1811–1812 New Madrid earthquake sequences, and the 1886 Charleston earthquake, and found that remotely triggered earthquakes tends to occur at sites known to be seismically active during historic times. Their results, together with our observation in the aftershock zone of the 1976 Tangshan earthquake, suggest that regions with elevated background seismicity rates (such as the aftershock zones of previous large earthquakes) are more susceptible to dynamic triggering, most likely because these areas contain nucleation points more frequently closer to failure (e.g., Hill *et al.*, 1993; Hough *et al.*, 2003; Hill and Prejean, 2007; Savage and Marone, 2008). However, we did not find clear triggering effects within the aftershock zone of the 1975 Haicheng earthquake, suggesting that high background seismicity would help, but is not the only condition for triggering to occur.

In all three cases, the most clear triggering effect is observed at stations NKY and DHC about 35 km SW of Beijing. This region defines a distinct lateral variation of lithospheric thickness that coincides with the major boundary between the Taihang Mountain to the west and the Bohai Bay Basin to the east (Chen *et al.*, 2008). Several major parallel faults, such as the Babaoshan and Huangzhuang-Gaoliying faults, cut across this region. Both stations are very close to these active faults. This region is also seismically active in historic times, with several M 6–7 earthquakes occurred in the 17–18th century (e.g., a $M\sim6.0$ event on 1658/02/03 and a $M\sim6.5$ on 1730/09/30). However, currently this region is seismically quiet, with on average 23 $M>1$ events each year since 2000. Although we were unable to locate the 4 events occurred during the large-amplitude surface waves, the short S–P times (less than 2 s) observed at station NKY suggest that these triggered earthquakes probably occurred directly on or very close to these parallel faults. Based on the network of leveling, gravity and geomagnetic observations, several studies have suggested that the Babaoshan fault is creeping (at least in the near surface), while the Huangzhuang-Gaoliying fault is currently locked (e.g., Che *et al.*, 1997). At this stage, the relationship between the triggered activity and fault behaviors are still not clear. If the triggered earthquake is associated with the locked Huangzhuang-Gaoliying fault, our observation may suggest that this region is critically stressed and close to fail in future seismic events (e.g., Zoback and Zoback, 2002; Hough *et al.*, 2003).

Many physical models have been proposed to explain how relatively small-amplitude seismic waves can triggered earthquakes at teleseismic distances (Hill and Prejean, 2007; and references therein). We are unable to identify or favor any physical model over others in this study, due to the relatively small number and short duration of observations. We note that our study area is not associated any geothermal or volcanic activities, suggesting that the triggering mechanism does not require conditions that is unique to these areas (e.g., movement of magmas). This is consistent with the recent results by Gomberg *et al.* (2004) and Velasco *et al.* (2008), suggesting that dynamic triggering is a ubiquitous phenomenon and can occur in a wide range of tectonic environments. However, we observed only a few triggered earthquakes during and immediately after the passage of teleseismic waves, as compared with swarm-like character of triggered events in geothermal and volcanic regions (e.g., Hill *et al.*, 1993; Prejean *et al.*, 2004). Hence, if the triggering mechanisms and necessary conditions were similar in all these regions, the conditions would be more abundant in geothermal and volcanic regions. Possible candidates include elevated fluid pressures, intensive faults and fractures, elevated background seismicity, or a combination of them.

If we assume plane wave propagation for teleseismic waves, the peak dynamic stress σ_d is proportional to $G\dot{u}/v_s$ (Jaeger and Cook, 1979), where G is the shear modulus, $\dot{u}$ is the peak ground velocity, and v_s is the phase velocity. The peak ground velocity measured from the instrument corrected vertical seismograms in this region is 1–2 cm/s. Using a nominal G value of 30 GPa, and $v_s = 3.5$ km/s for the Rayleigh waves, we estimate the dynamic stress to be 0.085–0.17 MPa. This is within the range of the dynamic stresses (roughly 0.01 to 0.3 MPa) obtained from previous studies of remote triggering of microearthquakes (e.g., Gomberg *et al.*, 2004; Prejean *et al.*, 2004).

It is interesting to note that none of the identified events are listed in the earthquake catalog compiled by the regional seismic network around the study region, and there is no clear change in seismicity rate within 30 days before and after the Wenchuan earthquake. Hence, based on catalog information alone, one would conclude that no earthquakes are triggered by the Wenchuan earthquake in this region. Similar patterns are observed in California and Pacific Northwest after the 2002 M_w 7.8 Denali Fault earthquake (Gomberg *et al.*, 2004; Prejean *et al.*, 2004), suggesting the importance of analyzing continuous seismic recordings for studying remotely triggered earthquakes.

In light of recent discovery of triggered non-volcanic tremor along the subduction zones in southwest Japan (e.g., Miyazawa and Mori, 2006) and Pacific northwest (Rubinstein *et al.*, 2007), and along the San Andreas fault system in California (Gomberg *et al.*, 2008; Peng *et al.*, 2008), we also examined all the data in our study region for possible evidence of triggered tremor. While we saw some elevated tremor-like signals during and immediately after the passage of teleseismic waves, the signals were not coherent among nearby stations and sometimes existed before the *P* waves of the Wenchuan earthquake. So far we have not find any clear evidence of triggered tremor in this region. We are also in the process of conducting a global survey of triggered earthquakes and non-volcanic tremor associated with the Wenchuan earthquake (Jiang *et al.*, 2008), and the results will be reported elsewhere.

Acknowledgments. We thank the CEA network center for providing data used in this study. ZP is supported by the National Science Foundation (grant EAR-0809834) and Georgia Tech College of Science Faculty Research Development Grant. The manuscript benefited from valuable comments by the guest editor Dr. Chuanzhen Zhu and the anonymous reviewers. WW and QFC are supported by National Natural Science Foundation of China (grant 40504007). TJ is supported by the "China Young Faculty Scholarship" from the China Scholarship Council.

References

Brodsky, E. E., V. Karakostas, and H. Kanamori, A new observation of dynamically triggered regional seismicity: earthquakes in Greece following the August, 1999 Izmit, Turkey earthquake, *Geophys. Res. Lett.*, **27**, 2741–2744, 2000.

Burchfiel, B. C., L. H. Royden, R. D. van der Hilst, B. H. Hager, Z. Chen, R. W. Kingc, C. Li, J. Lüc, H. Yao, and E. Kirby, A geological and geophysical context for the Wenchuan earthquake of 12 May 2008, Sichuan, People's Republic of China, *GSA Today*, **18**, 4–11, 2008.

Che, Z., Y. Gong, S. Liu, T. Liu, and G. Meng, Comprehensive study of fault activity of the Huangzhuang-Gaoliying and Babaoshan Fault in the middle section, *Earthquake Res. China*, **13**, 330–337, 1997.

Chen, Q.-F., Y. Chen, and L. Li, China digital seismic network improves coverage and quality, *Eos Trans. AGU*, **87**(30), doi:10.1029/2006EO300003, 2006.

Chen, L., T. Wang, L. Zhao, and T. Y. Zheng, Distinct lateral variation of lithospheric thickness in the northeastern North China Craton, *Earth Planet. Sci. Lett.*, **267**, 56–68, 2008.

Deng, Q., P. Zhang, Y. Ran, X. Yang, W. Min, and Q. Chu, Basic characteristics of active tectonics of China, *Sci. China Ser. D-Earth Sci.*, **46**, 356–372, 2003.

Freed, A. M., Earthquake triggering by static, dynamic, and postseismic stress transfer, *Ann. Rev. Earth Planet. Sci.*, **33**, 335–367, 2005.

Gomberg, J., P. A. Reasenberg, P. Bodin, and R. Harris, Earthquakes triggering by seismic waves following the Lander and Hector Mine earthquakes, *Nature*, **411**, 462–465, 2001.

Gomberg, J., P. Bodin, K. Larson, and H. Dragert, Earthquakes nucleated by transient deformations caused by the *M* 7:9 Denali, Alaska, earthquake, *Nature*, **427**, 621–624, 2004.

Gomberg, J., J. L. Rubinstein, Z. Peng, K. C. Creager, and J. E. Vidale, Widespread triggering of non-volcanic tremor in California, *Science*, **319**, 173, doi: 10.1126/science.1149164, 2008.

Hill, D. P. and S. G. Prejean, Dynamic triggering, in *Treatise on Geophysics*, 257–292, edited by Schubert, G., Vol. 4, *Earthquake Seismology*, edited by Kanamori, H., Elsevier, Amsterdam, 2007.

Hill, D. *et al.*, Seismicity remotely triggered by the magnitude 7.3 Landers, California, earthquake, *Science*, **260**, 1617–1623, 1993.

Hough, S. E. and H. Kanamori, Source properties of earthquakes near the Salton Sea triggered by the 16 October, 1999 *M* 7.1 Hector Mine earthquake, *Bull. Seismol. Soc. Am.*, **92**, 1281–1289, 2002.

Hough, S. E., L. Seeber, and J. G. Armbruster, Intraplate triggered earthquakes; observations and interpretation, *Bull. Seismol. Soc. Am.*, **93**, 2212–2221, doi:10.1785/0120020055, 2003.

Jaeger, J. C. and N. G. W. Cook, *Fundamentals of rock mechanics*, 3rd ed., Chapman and Hall, New York, 1979.

Jiang, T., Z. Peng, W. Wang, and Q.-F. Chen, Global survey of earthquakes and non-volcanic tremor triggered by the 2008 M_w 7.9 Wenchuan earthquake, *Eos Trans. AGU*, **89**(53), Fall Meet. Suppl., Abstract S23E-08, 2008.

Kilb, D., J. Gomberg, and P. Bodin, Aftershock triggering by complete Coulomb stress changes, *J. Geophys. Res.*, **107**(B4), 2060, doi:10.1029/2001JB000202, 2002.

Li, L., Q.-F. Chen, and Y. Chen, Relocated seismicity in big Beijing area and its tectonic implication, *Prog. Geophys.*, **2**, 24–34, 2007.

Liu, M., Y. Yang, Z.-K. Shen, S. Wang, M. Wang, and Y. Wan, Active tectonics and intracontinental earthquakes in China: The kinematics and geodynamics, in *Continental Intraplate Earthquakes: Science, Hazard, and Policy Issues*, edited by S. Stein and S. Mazzotti, 209–318, doi: 210.1130/2007.2425 (19), *Geol. Soc Am. Special Papers*, Boulder, CO, 2007.

Matthews, M. V. and P. A. Reasenberg, Statistical methods for investigating quiescence and other temporal seismicity patterns, *Pure Appl. Geophys.*, **126**, 357–372, 1988.

Miyazawa, M. and J. Mori, Evidence suggesting fluid flow beneath Japan due to periodic seismic triggering from the 2004 Sumatra-Andaman earthquake, *Geophys. Res. Lett.*, **33**, L05303, doi:10.1029/2005GL025087, 2006.

Peng, Z., J. E. Vidale, M. Ishii, and A. Helmstetter, Seismicity rate immediately before and after main shock rupture from high-frequency waveforms in Japan, *J. Geophys. Res.*, **112**, B03306, doi:10.1029/2006JB004386, 2007.

Peng, Z., J. E. Vidale, K. C. Creager, J. L. Rubinstein, J. Gomberg, and P. Bodin, Strong tremor near Parkfield, CA excited by the 2002 Denali Fault earthquake, *Geophys. Res. Lett.*, **35**, L23305, doi:10.1029/2008GL036080, 2008.

Prejean, S. G. *et al.*, Remotely triggered seismicity on the United States West Coast following the M_w 7.9 Denali Fault earthquake, *Bull. Seismol. Soc. Am.*, **94**, S348–S359, 2004.

Reasenberg, P. A. and R. W. Simpson, Response of regional seismicity to the static stress change produced by the Loma Prieta earthquake, *Science*, **255**, 1687–1690, 1992.

Rubinstein, J. L., J. E. Vidale, J. Gomberg, P. Bodin, K. C. Creager, and S. D. Malone, Non-volcanic tremor driven by large transient shear stresses, *Nature*, **448**, 579–582, 2007.

Savage, H. M. and C. Marone, Potential for earthquake triggering from transient deformations, *J. Geophys. Res.*, **113**, B05302, doi:10.1029/2007JB005277, 2008.

Shedlock, K. M., J. Baranowski, W. Xiao, and X. L. Hu, The Tangshan aftershock sequence, *J. Geophys. Res.*, **92**, 2791–2803, 1987.

Utsu, T., Y. Ogata, and R. S. Matsu'ura, The centenary of the Omori formula for a decay law of aftershock activity, *J. Phys. Earth*, **43**(1), 1–33, 1995.

Velasco, A. A., S. Hernandez, T. Parsons, and K. Pankow, Global ubiquity of dynamic earthquake triggering, *Nature Geosci.*, **1**, 375–379, doi:10.1038/ngeo204, 2008.

Wang, K., Q.-F. Chen, S. Sun, and A. Wang, Predicting the 1975 Haicheng earthquake, *Bull. Seismol. Soc. Am.*, **96**(3), 757–795, doi: 10.1785/0120050191, 2006.

Wang, Q., P.-Z. Zhang, J. T. Freymueller, R. Bilham, K. M. Larson, X. Lai, X. You, Z. Niu, J. Wu, Y. Li, J. Liu, Z. Yang, and Q. Chen, Present-day crustal deformation in China constrained by Global Positioning System (GPS) measurements, *Science*, **294**, 574–577, doi:10.1126/science.1063647, 2001.

Woessner, J. and S. Wiemer, Assessing the quality of earthquake catalogues: estimating the magnitude of completeness and its uncertainty, *Bull. Seismol. Soc. Am.*, **95**, 684–698, 2005.

Zoback, M. D. and M. L. Zoback, State of stress in the Earth's lithosphere, in *International Handbook of Earthquake and Engineering Seismology, Part A*, edited by W. H. K. Lee, H. Kanamori, P. C. Jennings, and C. Kisslinger, 559–568, Amsterdam, Academic Press, 2002.

Z. Peng (e-mail: zpeng@gatech.edu), W. Wang, Q.-F. Chen, and T. Jiang